Proton NMR Studies of Cytochrome *c* Peroxidase Mutant N82A: Hyperfine Resonance Assignments, Identification of Two Interconverting Enzyme Species, Quantitating the Rate of Interconversion, and Determination of Equilibrium Constants†

Steve L. Alam,‡ James D. Satterlee,*,‡ J. Matthew Mauro,§ Thomas L. Poulos,|| and James E. Erman⊥

Department of Chemistry, Washington State University, Pullman, Washington 99164-4630, Geo-Centers, Inc., Fort Washington, Maryland 20744 , Department of Molecular Biology & Biochemistry and Department of Physiology & Biophysics, University of California, Irvine, California 92717, and Department of Chemistry, Northern Illinois University, DeKalb, Illinois 60115

Received May 30, 1995; Revised Manuscript Received September 19, 1995⊗

ABSTRACT: The cyanide-ligated form of the baker's yeast cytochrome c peroxidase mutant bearing the mutation Asn82 → Ala82 ([N82A]CcPCN) has been studied by proton NMR spectroscopy. This mutation alters an amino acid that forms a hydrogen bond to His52, the distal histidine residue that interacts in the heme pocket with heme-bound ligands. His52 is a residue critical to cytochrome *c* peroxidase's normal function. Proton hyperfine resonance assignments have been made for the cyanide-ligated form of the mutant by comparison with 1-D and NOESY spectra of the wild-type native enzyme. For [N82A]CcPCN, proton NMR spectra reveal two significant phenomena. First, similar to results published for the related mutant [N82D]CcPCN [Satterlee, J. D., et al. (1994) *Eur. J. Biochem. 224*, 81−87], the Ala82 mutation disrupts the hydrogen bond between His52 and the heme-ligated CN. Second, four of the 24 resolved hyperfine-shifted resonances are doubled in the mutant enzyme's proton spectrum, leading to the concept that the heme active site environment is dynamically microheterogeneous on a very localized scale. Two magnetically inequivalent enzyme forms are detected in a pure enzyme preparation. Varying temperature causes the two enzyme forms to interconvert. Magnetization transfer experiments further document this interconversion between enzyme forms and have been used to determine that the rate of interconversion is 250 (±53) s^{-1}. The equilibrium constant at 20 °C is 1.5. Equilibrium constants have been calculated at various temperatures between 5 and 29 °C leading to the following values: $\Delta H = 60$ kJ mol^{-1}; $\Delta S = 0.20$ kJ K^{-1} mol^{-1}.

Cytochrome *c* peroxidase from baker's yeast (EC 1.11.1.5; CcP[1]) is a native ferriheme enzyme that catalyzes the ferrocytochrome *c* decomposition of hydrogen peroxide. Although there is some controversy surrounding the precise mechanistic details of this enzymatic reaction, eqs 1 and 2 express the essence of the process:

$$CcP(Fe^{3+})(Trp) + H_2O_2 \rightarrow CcPI(Fe^{4+}{=}O)(Trp^{\bullet}) + H_2O \quad (1)$$

$$CcPI(Fe^{4+}{=}O)(Trp^{\bullet}) + 2Cytc(Fe^{2+}) + 2H^+ \rightarrow CcP(Fe^{3+})(Trp) + 2Cytc(Fe^{2+}) + H_2O \quad (2)$$

From a combination of crystallographic (Poulos et al., 1980, 1984; Poulos & Kraut 1980; Poulos & Finzel, 1984; Edwards & Poulos, 1990) and solution (Satterlee & Erman, 1991; Satterlee et al., 1994) studies, it is widely appreciated that both resting state wild-type native cytochrome *c* peroxidase (CcP) and cyanide-inhibited wild-type native cytochrome *c* peroxidase (CcPCN) possess an extensive and functionally important hydrogen-bonding network encompassing both proximal and distal sides of the heme active site. A similar conclusion has been made on the basis of similar results for the recombinant enzyme MKT-CcPCN (Banci et al., 1991). This hydrogen-bond network is considered important to the enzyme's role in hydrogen peroxide decomposition (Poulos & Kraut, 1980; Poulos & Finzel, 1984). However, the solution-state chemical and structural consequences of specifically mutating individual amino acids that contribute to the hydrogen-bond network are just starting to be revealed.

For the purposes of proton NMR spectroscopy the cyanide-ligated form of CcP (and its mutants) provides an excellent model of the low-spin paramagnetic enzyme intermediates, CcP-I and CcP-II, that occur in the enzyme's reaction cycle (eqs 1 and 2; Poulos et al., 1980; Poulos & Finzel, 1984;

† We acknowledge support for this research from the following agencies: National Institutes of Health (GM 47645, RR 0631401 to J.D.S.; .GM 42614 to T.L.P.) and the National Science Foundation (MCB9121414 to J.E.E.).

* Corresponding author: Department of Chemistry, Washington State University, Pullman, WA 99164-4630. Telephone: 509-335-8620. Fax: 509-335-8867. Internet: hemeteam@cosy.chem.wsu.edu.

‡ Washington State University.

§ Geo-Centers, Inc.

|| University of California.

⊥ Northern Illinois University.

⊗ Abstract published in *Advance ACS Abstracts,* November 1, 1995.

[1] Abbreviations CN, cyanide, refers to all forms of KCN in solution, both ligated and not; CcP, wild-type native cytochrome *c* peroxidase; CcPCN, wild-type native cyanide-ligated cytochrome *c* peroxidase; MKT-CcPCN, recombinant cyanide-ligated cytochrome *c* peroxidase with the extended sequence Met-Lys-Thr at the amino terminus.

0006-2960/95/0434-15496$09.00/0

Edwards & Poulos, 1990). CcPCN also has the spectroscopic advantage of having comparatively narrow proton hyperfine resonances, in contrast to the very broad, featureless spectrum of CcP-I and CcP-II (Satterlee & Erman, 1981, 1991). Accordingly, we have previously studied the cyanide-ligated form of the CcP mutant in which the naturally occurring asparagine at primary sequence position 82 was replaced by aspartic acid ([N82D]CcPCN; Satterlee et al., 1994). Here we report corresponding NMR results for the cyanide-ligated CcP mutant in which Asn82 is replaced by Ala ([N82A]CcPCN).

By focusing on single point mutations at position 82, we have been trying to elucidate the chemical consequences of changing an amino acid that indirectly interacts with the heme active site. Based upon the crystal structure of wild-type native CcP, it was concluded that in the wild-type native enzyme the side-chain carbonyl of Asn82 serves as a hydrogen-bond acceptor from His52 (Poulos et al., 1984; Poulos & Finzel, 1984; Edwards & Poulos, 1990). This structural feature is conserved in all of the published peroxidase structures (Edwards & Poulos, 1990; Poulos et al., 1993; Sundaramoorthy et al., 1994; Petersen et al., 1994; Kunishima et al., 1994; Patterson & Poulos, 1995). His52 is located in the heme pocket, on the distal side of the heme, and is the amino acid located closest to the ligand binding site. His52 is critical to proper enzyme catalysis and is proposed to interact as a hydrogen-bond partner with heme-bound hydrogen peroxide in order to facilitate its decomposition during enzyme functioning (Poulos & Kraut 1980; Poulos & Finzel, 1984). Spectroscopic studies provide evidence that His52 functions similarly, as a hydrogen-bond partner to heme-ligated CN, in native CcPCN (Satterlee & Erman, 1991; Satterlee et al., 1994). The point of this study, then, has been to determine the spectroscopic consequences manifested at the heme active site as a result of modifying the His52−amino acid 82 interaction by replacing Asn82 with Ala.

EXPERIMENTAL PROCEDURES

Oligonucleotide site-directed mutagenesis was carried out following the methods of Kunkel et al. (1987) in the cytochrome *c* peroxidase gene cloned into the PT7-7 vector (Darwish et al., 1991). N-terminal analysis of recombinant wild-type CcP expressed in this system indicated the presence of the expected N-terminal threonine residue. Isolation, chromatography, and purification of recombinant mutant enzyme was carried out according to Fishel et al. (1987). The wild-type native enzyme was isolated and purified from baker's yeast (Red Star) using previously described methods (Vitello et al., 1990; Summers & Erman, 1988). Both proteins were recrystallized twice by dialysis against distilled water.

The structure of native CcPCN (Poulos et al., 1984) was graphically displayed on a Silicon Graphics Indigo2 workstation using the program InsightII (Biosym Technologies). Figures 1B and 1C were generated by scanning the appropriate InsightII stereo output into Photoshop (Adobe Systems) running on an Apple PowerMacintosh 7100, where labels were added prior to final printing.

Protein samples were prepared for NMR spectroscopy in a "D_2O/buffer" solution consisting of D_2O (99.9 atom % D; Isotec), 75 mM potassium phosphate (Fisher Certified), and 100 mM potassium nitrate (Fisher), pH′ = 6.4 (uncorrected meter reading in the D_2O/buffer solution). The pH′ was measured with a calibrated Fisher combination electrode and a Fisher 925 meter. Cyanide ligation was carried out by adding a 10% mole excess of potassium cyanide (Fisher) from a freshly made stock solution of KCN in 99.9% D_2O. The pH′ of NMR sample solutions was adjusted either with DCl or NaOD (both MSD Isotopes) when required.

Proton 1D absorption NMR spectra were obtained on a Varian VXR500s spectrometer operating at the nominal proton frequency of 500 MHz, as previously described (Satterlee et al., 1994; Satterlee & Erman, 1991). In 1-D spectra, as in Figures 2 and 3, baseline straightening was employed. The probe temperature was calibrated with a sealed, degassed methanol sample. One-dimensional experiments were carried out using 8−16K data points over a 19 kHz spectral band width (CcPCN), with typical recycle times of 0.60 s, employing 7−10 μs $\pi/2$ pulse widths. 1-D data were processed with 5−30 Hz line broadening.

Saturation-transfer (Sandstrom, 1982; Yi et al., 1994) experiments were carried out using the spectrometer's B-frequency channel as the irradiation source, by carefully adjusting the power level and duration so as to minimize unintended irradiation of neighbor peaks (called "spillover"). Inversion-transfer experiments were implemented using a semiselective on-resonance sequence: $\pi/2-t-\pi/2-\tau_{ex}-\pi/2-$obs (Yi et al., 1993, 1994), where τ_{ex} is the variable-time increment during which chemical exchange transfers magnetization between the two different environments. The inversion-transfer data were analyzed using either exhaustive brute-force five-parameter fitting protocol or a Monte-Carlo/least squares three-parameter fitting protocol (Yi et al., 1994). Our implementation of these magnetization-transfer experiments, along with the data analysis procedure, has been described in detail elsewhere (Yi et al., 1993, 1994; Erman & Satterlee, 1995).

Phase-sensitive NOESY spectra were obtained using the method of States et al. (1982), as previously described for CcPCN (Satterlee & Erman, 1991) and [N82D]CcPCN (Satterlee et al., 1994). Typical experimental parameters used were 1024 points in t_2 × 256 t_1 increments, 96 pulses/increment, and mixing times between 0.6 and 70 ms with decoupler suppression of any residual water resonance. 2-D data were processed to 2K × 2K final matrix sizes using either sine-bell or sine-squared apodization functions. Typically these data sets were not symmetrized.

Peak integrations were determined repetitively (n = 10) by plotting the expanded peak regions, deconvoluting the peaks, cutting out the broad peaks, and weighing them on a Mettler microbalance. This was done redundantly for spectra with and without baseline straightening (Figure 2B). The error of reproducibility in these integrations translates into an error in proton counting, which is ±18%.

There is evidence in the NMR spectra of the recombinant mutant protein of slight amounts of CcP-related heterogeneity in addition to the major dual-peak heterogeneity studied in this work. This is indicated in Figures 2 and 3 as barely detectable small peaks in the 22−25 ppm region. In view of the demonstrated purity of the mutant protein as assayed by SDS−PAGE (one band appears), we believe that this very minor form (or forms) is a derivative of the parent enzyme which encompasses yet another conformation. Similar results were encountered in studies of the related [N82D]-

CcPCN mutant (Satterlee et al., 1994). The presence of this minor form does not compromise the experiments and conclusions made in this study for the predominant parent mutant enzyme.

RESULTS AND DISCUSSION

With respect to the following discussion, Figure 1A presents the heme and histidine labeling schemes that we have used in this work. With respect to the heme, we have previously noted that this is a modified Fischer labeling scheme, with the heme pyrrole rings labeled A−D (Satterlee & Erman, 1991). Figure 1 panels B and C are structural representations of the heme environment in wild-type native CcPCN derived from X-ray crystallography (Poulos et al., 1984; Edwards & Poulos, 1990). Both Figure 1 panels B and C present views looking onto the heme from an approximately perpendicular vantage point situated at the distal (ligand binding) side of the heme. Figure 1B shows several distal-side amino acids in the native CcPCN heme pocket, while Figure 1C shows several proximal-side amino acids.

Proton Resonance Heterogeneity. Proton NMR spectra of wild-type CcPCN and [N82A]CcPCN are compared in Figure 2. The protein solutions were identical (see Experimental Procedures). The peak by peak correspondence between these two spectra in the high frequency region (between 11 and 32 ppm) is readily recognized if it is accepted (as will be demonstrated) (i) that three resonances of CcPCN (nos 1, 5 and 8; Figure 2A) appear doubled in [N82A]CcPCN (1/1′, 5/5′, and 8/8′; Figure 2B) and (ii) that resonance 10 (His52 C_2H) is completely missing from the [N82A]CcPCN spectrum. This latter point is critical to interpreting the [N82A]CcPCN spectra. Further evidence supporting both these points will be presented. The observed shifts and assignments derived from this correlation and the NOE data (discussed later) are given in Table 1.

In the low frequency region between −1 and −5 ppm (Figure 2B) there is, at first glance, little obvious correspondence between the mutant and native enzymes. However, careful comparison reveals that resonance 24 (assigned to Arg48 at ~−4.2 ppm in Figure 2A) has an apparently corresponding doubled resonance (nos 24/24′) in Figures 2 and 3.

The pattern of [N82A]CcPCN proton hyperfine shifts is highly temperature dependent as shown in Figure 3. First, there is the general temperature dependence (Curie behavior) exhibited by hyperfine-shifted resonances in paramagnetic molecules (Satterlee, 1986). Second, by focusing on the peak pairs labeled 1/1′, 5/5′, 8/8′, and 24/24′ in Figure 3, one can trace a temperature-dependent intensity interconversion within each pair. This is especially obvious for the 1/1′ pair of resonances, which appear well resolved from neighbor resonances throughout the temperature range. At 5 °C in our D_2O/buffer solution at pH′ 6.4 the peaks labeled 1, 5, 8, and 24 predominate. At 29 °C the 1′, 5′, 8′, and 24′ peaks predominate. Within experimental error the combined relative integrated intensity of each pair remains constant throughout the temperature range. This points to an equilibrium between two enzyme forms, distinguished by the unprimed and primed numbers. Those relative intensities, normalized to the three-proton intensity of the heme 8-CH_3 resonance (peak 3), or to the one-proton intensity His175 NpH resonance (peak 11), are as follows: 1/1′ = 3 protons; 5/5′ = 8/8′ = 24/24′ = 1 proton. Of the 24 resolved hyperfine-shifted resonances shown in Figure 2, only four resonances are detectably doubled in the mutant at this magnetic field strength and also display the pairwise intensity ratio changes demonstrated in Figure 3. As judged by the similar NMR shifts of the two forms, the differences between them are not indicative of global conformational differences. Rather, at the level of the present data the magnetic inequivalence appears to be localized to a specific region of the heme active site. This point will be developed further in the following analysis.

Proton Resonance Assignments. Making unambiguous assignments of the hyperfine shifted resonances was critical to understanding the solution behavior of this mutant enzyme. A set of proton resonance assignments (Table 1) that are consistent with those elucidated for wild-type native CcPCN have been made by an extensive comparison of the 1-D and NOESY spectra of native CcPCN and [N82A]CcPCN at various temperatures. These results have also provided supporting data for the concept that two slightly different enzyme forms are present in D_2O/buffer solutions at pH′ 6.4.

Established assignments for native CcPCN (Satterlee & Erman, 1991) MKT-CcPCN (Banci et al., 1991) and [N82D]-CcPCN (Satterlee et al., 1994) provided the basis for interpreting the proton homonuclear NOESY connectivities obtained here for [N82A]CcPCN. Typical results are shown in Figures 4 and 5. A representative contour plot of NOESY data taken at 5 °C (15 ms mixing time) is shown in Figure 4 and the cross peak assignments are given in the caption. Data taken at the same temperature with both 30 and 40 ms mixing times are similar, although cross peaks display the expected mixing time dependence of intensity (data not shown). In comparison with very extensive unpublished NOE studies on wild-type native CcPCN obtained in this laboratory, no unusual NOE data were found for [N82A]-CcPCN. The temperature of 5 °C was initially chosen so that one form of the enzyme would predominate, thereby simplifying the initial interpretation of the cross peak connectivity pattern. For simplicity, only the regions of the data relevant to the hyperfine shift assignments are presented in Figures 4 and 5. The cross peak connectivity pattern shown in Figure 4 is virtually identical to those for native CcPCN (Satterlee et al., 1991), MKT-CcPCN (Banci et al., 1991), and [N82D]CcPCN (Satterlee et al., 1994), and, for example, one can easily identify the cross peaks of His175 and the heme 7-propionate. This consistency with the previous CcPCN data leads, straightforwardly, to the assignments presented in the caption.

Figure 5 presents a corresponding NOESY contour plot for an experiment carried out at 20 °C (40 ms mixing time) with assignments also given in the caption. At this temperature in the D_2O/buffer solution at pH′ 6.4 there is a nearly equal mixture of the two enzyme forms (Figure 3), which complicates the spectral analysis. For example, the divided intensity of the individual doubled peaks in the pairs 5/5′, 8/8′, and 24/24′ renders their detection difficult with our present instrumentation. Of the four resonances 5/5′ and 8/8′, only the 5′ is detectable on the contour plot diagonal at the contour level displayed in Figure 5. However, cross peaks due to both resonances 5 and 5′ appear as pairs j/j′ and k/k′ in Figure 5, and, among others, one can readily identify the cross peak connectivities of His175 and (for both enzyme

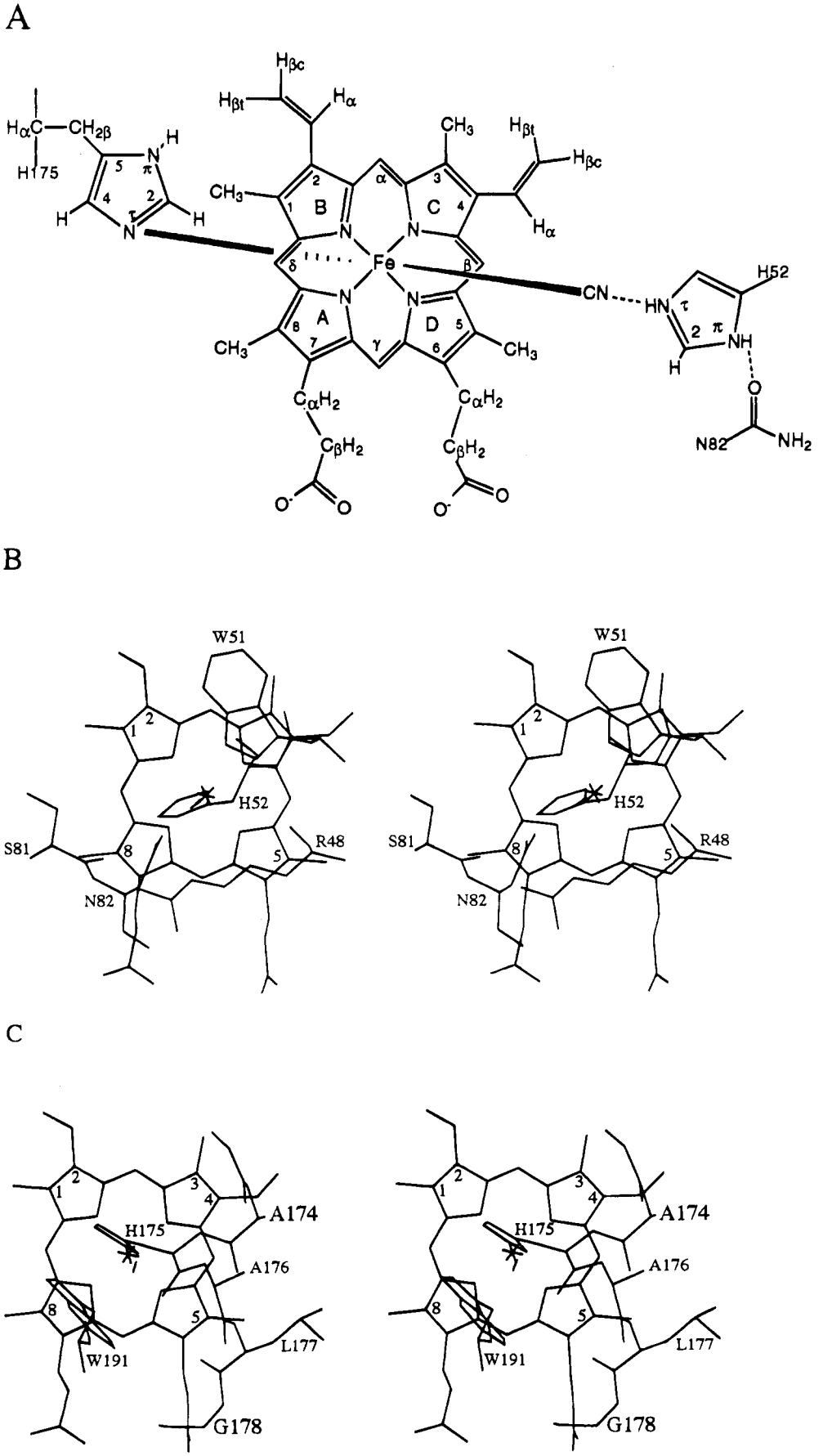

FIGURE 1: (A) Heme and histidine labeling. (B) Stereoview of the native CcPCN heme pocket. View is perpindicular to the heme from the distal side. Distal amino acids closest to the heme are labeled. Heme pyrrole positions 1, 2, 5, and 8 are labeled for reference to panel A. The heme iron ion is depicted as a star at the heme center, and the coordinated CN is shown as straight line situated between His52 and the heme iron ion. (C) Stereoview similar to panel B except that only proximal amino acids along the helical segment corresponding to primary sequence 173−178 are shown, along with Trp191. The label for Gly 173 is omitted.

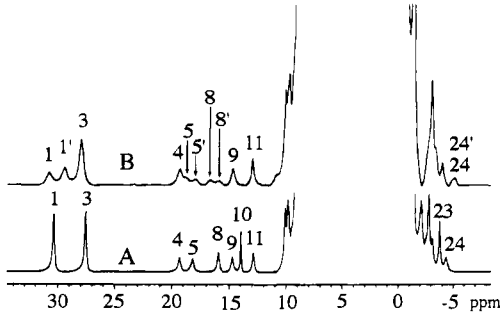

FIGURE 2: 500 MHz proton NMR spectra of wild-type native CcPCN (A) and [N82A]CcPCN (B). Resonances are numbered for identification in the text and Table 1 as in Satterlee et al. (1994). Solution conditions: 20 °C, pH′ 6.4, 75 mM potassium phosphate/100 mM potassium nitrate, in D_2O. Baseline straightening was applied to both spectra.

Table 1: Observed Proton NMR Shifts and Tentative Assignments for [N82A]CcPCN in Comparison to Wild-Type CcPCN

peak[a]	assignment	Observed Shift[b] [N82A]	[wild type]
1	$3CH_3$	30.9	30.9
1′	$3CH_{3'}$	29.5	
3	$8CH_3$	28.0	27.8
4	His175βH	19.4	19.7
5	heme 7αH	18.9	18.5
5′	heme 7αH	18.0	
8	heme 4αH	16.6	16.0
8′	heme 4αH	15.9	
9	His175βH	14.7	15.0
10	His52C_2		14.0
11	His175NpH	13.0	13.0
	His 175αH	8.63	8.48[c]
	Leu232δCH_3	2.99; −1.22	2.91; −1.19
	heme 7αH[d]	6.38	6.24[c]
	heme 7β	−1.30	−1.52
	heme 4β	−0.22 (?)	−4.00; −2.24

[a] Labels correspond to Figure 2. [b] Reported in ppm for both proteins at 20 °C, pH′ = 6.40, 0.10 M potassium nitrate/0.075 M potassium phosphate, referenced to residual HDO at 4.70 ppm. [c] Shifts at 22 °C reported in Satterlee and Erman (1991). [d] The geminal partner to resonance 5.

forms) the heme 7-propionate. Other NOESY experiments were carried out at various mixing times between 0.6 and 70 ms (20 °C), as well as at different temperatures, both to aid in assignments and to provide a complete data base of cross peak intensities as a function of mixing time (NOE buildup). Specifically, the extensive NOESY data at 20 °C were also used to quantitate the dynamic rate of interconversion between the two [N82A]CcPCN enzyme forms.

Relationship between Wild-Type and Mutant Enzyme Spectra. The spectral data presented in Figures 2−5 show that no resonance with characteristics of the His52 C_2H (peak no. 10 in native CcPCN, Figure 2A) is found in the hyperfine shift region of the mutant (Figure 2B). The conclusion that this peak is absent from the hyperfine shift region in [N82A]-CcPCN is further supported by the NOESY data. In wild-type CcPCN the His52 C_2H resonance is unique. Not only is it highly identifiable by its unique narrowness, it is the most slowly relaxing of the hyperfine-shifted proton resonances, and, among all of these resonances, it lacks discernible NOESY cross peaks when mixing times under 50 ms are employed (Satterlee & Erman, 1991). With these criteria and the intensity integrations described above, no resonance in the NOESY spectra could be assigned to His52 C_2H. This

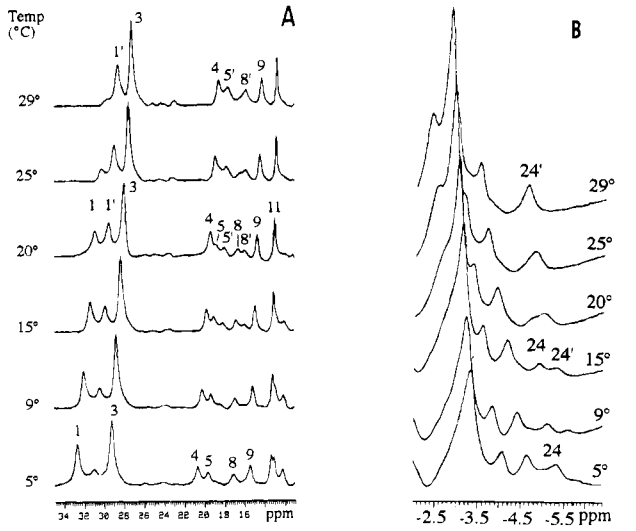

FIGURE 3: Effect of varying temperature on the high frequency (A) and low frequency (B) proton hyperfine shift regions. Spectra were taken at 500 MHz. Other solution conditions identical to those described in the Figure 2 caption. Peak labels correspond to Figure 2.

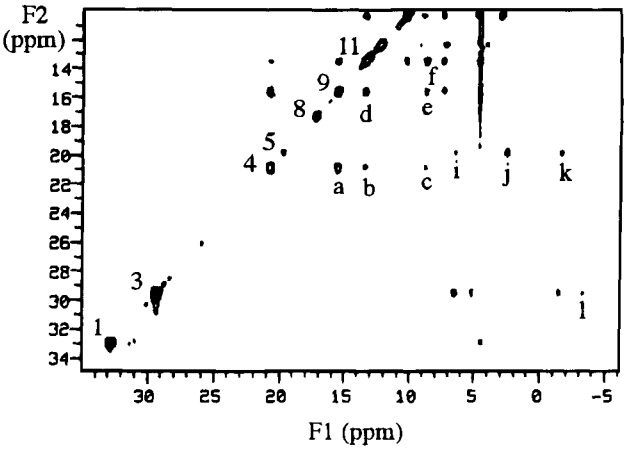

FIGURE 4: Unsymmetrized 500 MHz homonuclear proton NOESY contour plot of [N82A]CcPCN at 5 °C (mixing time = 15 ms). Only part of the total spectrum is shown. Solution conditions were as described in the Figure 2 caption. Diagonal peak labels correspond to Figure 2. Cross peak assignments: (a) His175β/β; (b) His175β/NpH; (c) His175β/α; (d) His175β/NpH; (e) His175β/α; (f) His175NpH/α; (g) heme 4α/4β(cis); (i) heme 7α/7α; (j) heme 7α/γ meso; (k) heme 7α/7β; (l) heme 8-CH_3/Leu232 δCH_3.

result is identical to proton NMR results reported previously for the related mutant enzyme [N82D]CcPCN which revealed that replacement of Asn82 by Asp resulted in loss of the His52-ring proton resonances from the hyperfine shift region (Satterlee et al., 1994).

Movement of the His52 C_2H resonance out of the high-frequency hyperfine shift region for [N82D]CcPCN was interpreted as reflecting disruption of the His52−heme-coordinated CN hydrogen bond. The absence of an identifiable, hyperfine-shifted His52 C_2H for this mutant leads to the same conclusion, that the His52−heme-coordinated CN hydrogen bond is missing in [N82A]CcPCN. In the context of our previous work on [N82D]CcPCN this is a second example of how changing the position-82 amino acid has mediated the His52−heme ligand interaction. However, as we will demonstrate, the proton NMR spectum of [N82A]-CcPCN is significantly more interesting than was the

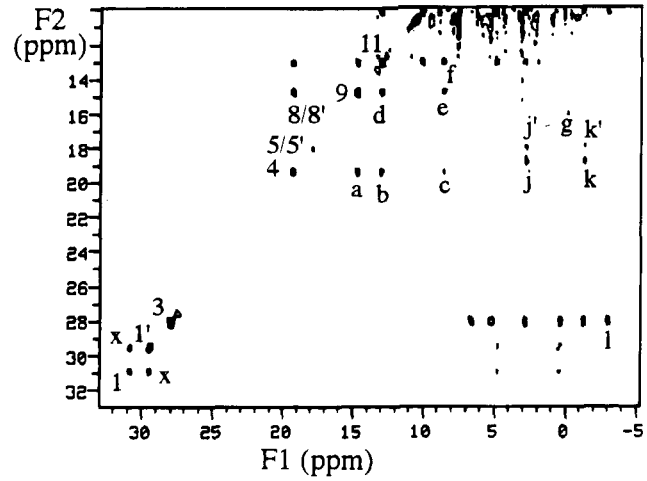

FIGURE 5: Unsymmetrized 500 MHz homonuclear proton NOESY contour plot of [N82A]CcPCN at 20 °C (mixing time = 40 ms). Only part of the total spectrum is shown. Solution conditions were as described in the Figure 2 caption. Diagonal peak labels correspond to Figure 2. Cross peak assignments: (x) exchange cross peak connecting the two heme 3-CH_3 resonances, 1/1′; (a) His175β/β; (b) His175β/NpH; (c) His175β/α; (d) His175β/NpH; (e) His175β/α; (f) His175NpH/α; (g) heme 4α/4β(cis); (j/j′) heme 7α/γ meso; (k/k′) heme 7α/7β; (l) heme 8-CH_3/Leu232 δCH_3. The diagonal peaks 8/8′ corresponding to the magnetically inequivalent heme 4-vinyl αH resonances are not detected at this contour level. At lower contour levels peak g′, the cross peak from 8′, is also detected.

spectrum of [N82D]CcPCN since there are two closely related, but NMR distinguishable enzyme species in solution.

Demonstrating the Dynamic Interconversion of the Two Enzyme Forms. Figure 5 is noteworthy because it reveals that there is a strong cross peak (labeled x) connecting corresponding peaks in each enzyme form, 1/1′. From the assignment data presented above we are certain that the 1/1′ peak pair corresponds to the heme $3CH_3/3CH_3'$. Accordingly, no NOE is expected between these resonances. The only explanation for this strong cross peak is that it is due to an exchange process in which the heme $3CH_3$ samples two inequivalent magnetic environments.

Unambiguous evidence for the pairwise exchange relatedness of the 1/1′, 5/5′, and 8/8′ peaks comes from magnetization transfer experiments (Sandstrom, 1982; Alger & Shulman, 1980; Spencer et al., 1993), as shown in Figures 6 and 7. Figure 6 reveals that, in saturation-transfer experiments, selective saturation can be achieved and spillover avoided. This is indicated by irradiation of the 1′ resonance with negligible perturbation of the neighbor heme 8-CH_3 resonance (peak 3 in Figure 6B). Figure 6B further shows that when resonance 1′ is irradiated, the exchange-related partner resonance (no. 1) experiences significant loss of intensity. The inverse irradiation experiment yielded identical results. Similar experiments directed at the 5/5′ and 8/8′ resonance pairs yielded similar results but were more ambiguous due to the closer overlap of these pairs. Nevertheless, those results are entirely consistent with the conclusion that each of these three pairs consists of exchange-related partners and, in combination with the variable temperature changes shown in Figure 3, provide additional support for the conclusion that a localized part of the enzyme heme pocket is undergoing a dynamic equilibrium between two magnetically inequivalent forms.

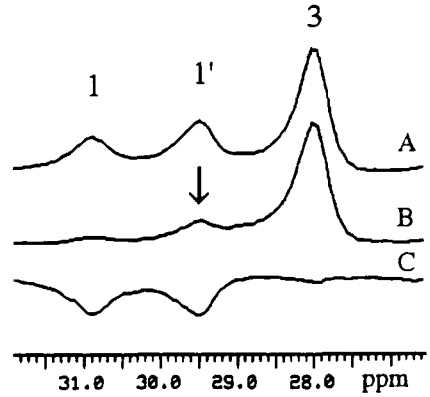

FIGURE 6: Saturation-transfer experiments for heme 3-CH_3 resonances (peaks 1/1′) of [N82A]CcPCN. Solution conditions as described in the Figure 2 caption. (A) "Off-resonance" irradiation; (B) "on-resonance" irradiation of peak 1′. (C) Difference spectrum, B − A. The lack of intensity for peak 8 in the difference spectrum illustrates the selectivity of the irradiation.

Quantitating the Lifetime of Each Enzyme Form. Another magnetization transfer experiment, inversion transfer (Figure 7; Sandstrom, 1982; Alger & Prestegard, 1977; Alger & Shulman, 1980; Spencer et al., 1993; Martin et al., 1980), was used to determine the dynamic lifetimes of the two enzyme species. Our implementation of this experiment and data analysis has been described previously in detail (Yi et al., 1993, 1994). Figure 7A shows one set of experimental data for the 1/1′ peak pair. Figure 7B shows the digitized peak-height data and the fits to the data that were obtained using our least squares method of analysis (Yi et al., 1994). The inversion-transfer data further confirmed the exchange relatedness of this pair of resonances. The pre-exchange lifetime of the enzyme form represented by resonance 1 was found to be 4.0 ± 0.7 ms. Since the process of interconversion between the two forms is a unimolecular process, the lifetimes of both forms are equal. In this situation the inverse of the lifetime yields a unimolecular rate constant of 250 (± 53) s^{-1}.

Equilibrium Constants. The two types of magnetization transfer experiments confirmed the fact that at least some regions of the heme active site consist of two different forms and that these two forms interconvert slowly on the NMR time scale. Consequently, it was straightforward to determine the equilibrium constant governing these two forms by integrating the deconvoluted individual peaks in each resonance pair (1/1′, 5/5′, and 8/8′) in order to estimate the relative concentrations of each enzyme form. The evidence presented above implicates a simple two-state equilibrium that is described by

$$[\text{N82A}]\text{CcPCN} = [\text{N82A}]\text{CcPCN}' \qquad (3)$$

In this definition the predominant low-temperature form of the enzyme that is characterized by the unprimed peaks (Figure 2) appears on the left of eq 1. The predominant enzyme form at high-temperature that is characterized by the primed peaks is designated with a prime and lies on the right of eq 1. Equilibrium constants (K_{eq}) were calculated for temperatures between 5 and 29 °C (Table 2). The thermodynamic parameters were estimated from a graph of ln K_{eq} against T^{-1} (Figure 8, correlation coefficient = 0.99) and are ΔH = 60 kJ mol^{-1} and ΔS = 0.20 kJ K^{-1} mol^{-1}.

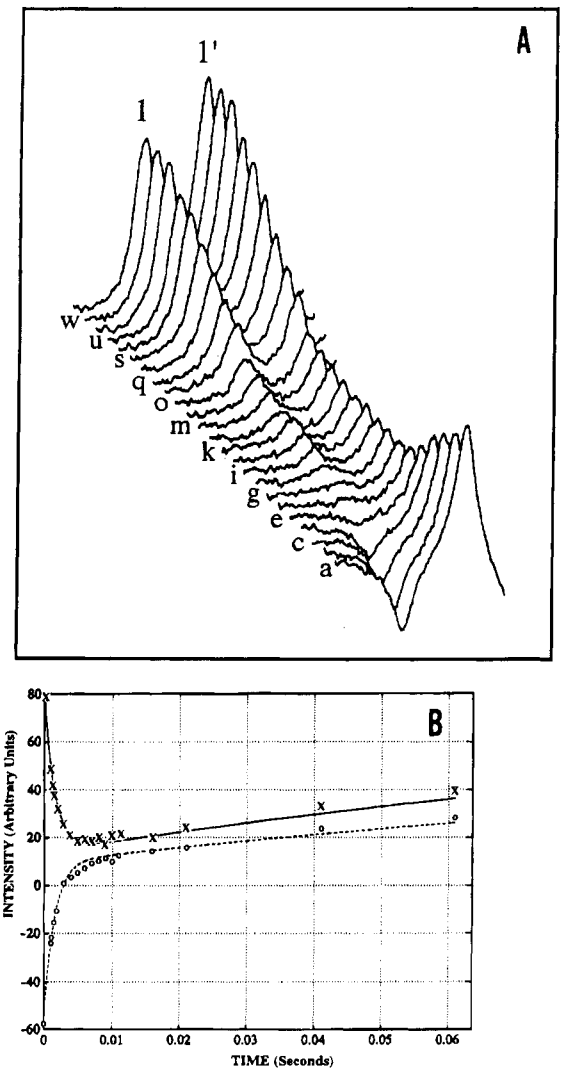

FIGURE 7: (A) Inversion-transfer experiment shown for the heme 3-methyl proton resonances (peaks 1/1′). Solution conditions were as described in the Figure 2 caption. Magnetization exchange times (s): (a) 0.000; (b) 0.0011; (c) 0.0015; (d) 0.0020; (e) 0.0030; (f) 0.0040; (g) 0.0050; (h) 0.0060; (i) 0.0070; (j) 0.0080; (k) 0.0090; (l) 0.010; (m) 0.011; (n) 0.016; (o) 0.021; (p) 0.041; (q) 0.061; (r) 0.101; (s) 0.201; (t) 0.601; (u) 1.001; (v) 3.001; (w) 6.001; (x) 10.001. (B) Plot of digitized peak intensities as a function of magnetization transfer times (s) with best-fit solutions indicated by lines drawn through the data points. Lower data set is for the inverted peak, no. 1; upper data set is for the exchange-related peak no. 1′.

Table 2: K_{eq} Dependence upon Temperature for [N82A]CcpCN[a]

K_{eq}	°C
5.6	29
2.8	25
1.5	20
0.98	15
0.65	9
0.46	5

[a] pH′ = 6.40, 0.10 M potassium nitrate/0.075 M potassium phosphate/D_2O. The error of reproducibility of K_{eq} values is estimated to be ±18% (see Experimental Procedures).

CONCLUSIONS

The data presented here have demonstrated the existence of two interconverting forms of [N82A]CcPCN in D_2O/buffer solutions at pH′ = 6.4, over the temperature range of 5−29 °C. The rate of interconversion between these two forms at 20 °C is ~250 s^{-1}, and the equilibrium constant at this temperature is 1.5. In wild-type native CcPCN no similar peak-doubling phenomenon is found under identical conditions. The two forms of [N82A]CcPCN are characterized by resolvable shift differences for four of the resolved proton hyperfine resonances, three of which are assignable to heme peripheral substituents on pyrroles A or C (Figure 1A). The shift data presented in Table 1 and the overall similarity of the wild-type native CcPCN and [N82A]CcPCN proton spectra suggest that no major structural disruption has occurred.

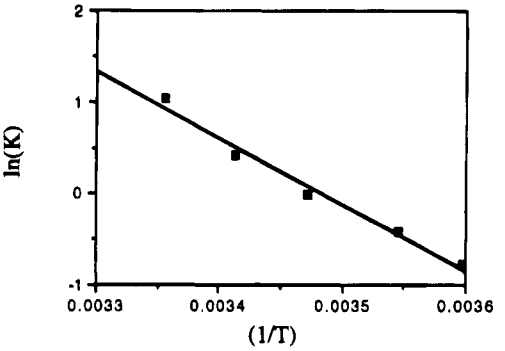

FIGURE 8: Temperature dependence of the equilibrium constant for the interconversion between two enzyme forms in [N82A]-CcpCN shown as a graph of ln K_{eq} plotted against T^{-1}.

The two enzyme forms in equilibrium involve regions in the heme pocket in such a way that only the heme peripheral substituents at the 3-, 4-, and 7-positions, and possibly part of the Arg48 residue, are affected. We hypothesize that the [N82A] mutation results not only in removal of the His52 hydrogen bond to heme-coordinated cyanide but that it also allows an increase in the conformational mobility of one or more amino acids in the heme pocket. This results in an equilibrium between two localized structural conformations.

The conformational heterogeneity observed may also be the result of more extensive disruption of the hydrogen-bonding network centered around His52 on the distal side of the heme. Figure 1B shows the distal amino acids closest to the heme and to the mutation site, Asn82. The Trp51, His52, Arg48, and Ser81 side chains are positioned such that movement by any one (or more) of them could be transmitted to the affected pyrrole areas of the heme. This would result in changes in heme−protein interactions and concomitant hyperfine shift changes.

Examination of the proximal side amino acids closest to the heme (Figure 1C) reveals no obvious pattern of interactions that would be situated so as to affect the pyrrole A and C substituents. We conclude that, most likely, structural rearrangement of certain amino acids on the distal side of the heme are responsible for the equilibrium heterogeneity. Since the His52−CN hydrogen bond is no longer present in the mutant, it seems reasonable to conclude that the origin of the conformational heterogeneity is the His52 imidazole side chain adopting one or more alternative positions. The observed small ΔS value is consistent with this. We continue to investigate this phenomenon.

REFERENCES

Alger, J. R., & Prestegard, J. H. (1977) *J. Magn. Reson. 27*, 137−141.

Alger, J. R., & Shulman, R. G. (1984) *Q. Rev. Biophys. 17*, 83−124.
Banci, L., Bertini, I., Turano, P., Ferrer, J. C., & Mauk, A. G. (1991) *Inorg. Chem. 30*, 4510−4516.
Bosshard, H. R., Anni, H., & Yonetani, T. (1991) in *Peroxidases in Chemistry and Biology* (Everse, J., Everse, K. E., & Grisham, M. B., Eds.) Vol. 2, pp 52−78, CRC Press, Boca Raton, FL.
Darwish, K., Li, H., & Poulos, T. L. (1991) *Protein Eng. 4*, 701−708.
Edwards, S. L., & Poulos, T. L. (1990) *J. Biol. Chem. 265*, 2588−2595.
Erman, J. E., & Vitello, L. B. (1980) *J. Biol. Chem. 255*, 6224−6337.
Erman, J. E., & Satterlee, J. D. (1995) *Adv. Biophys. Chem.* (in press).
Erman, J. E., Vitello, L. B., Miller, M. A., Shaw, A., Brown, K. A., & Kraut, J. (1993) *Biochemistry 32*, 9798−9806.
Fishel, L. A., Villafranca. J. E., Mauro, J. M., & Kraut, J. (1987) *Biochemistry 26*, 351−360.
Kunishima, N., Fukuyama, K., Matsubara, H., Hatanaka, H., Shibano, Y., & Amachi, T. (1994) *J. Mol. Biol. 235*, 331−344.
Kunkel, T. A., Roberts, J. D., & Zokour, R. A. (1987) *Methods Enzymol. 154*, 367−382.
Martin, J. L., Delpuech, J. J., & Martin, G. J. (1980) *Practical NMR Spectroscopy*, Heydon and Son Ltd., London.
Patterson, W. R., & Poulos, T. L. (1995) *Biochemistry 34*, 4331−4341.
Petersen, J. F., Kaziola, A., & Larsen, S. (1994) *FEBS Lett. 339*, 291−296.
Poulos, T. L., & Kraut, J. (1980) *J. Biol. Chem. 255*, 8199−8205.
Poulos, T. L., & Finzel, B. C. (1984) in *Peptide and Protein Reviews* (Hearn, M. T. W., Ed.) Vol. 5, pp 115−171, Marcel Dekker, New York.
Poulos, T. L., Freer, S. T., Alden, R. A., Edwards, S. L., Skogland, U., Takio, K., Eriksson, B., & Kraut, J. (1980) *J. Biol. Chem. 255*, 575−580.
Poulos, T. L., Finzel, B. C., & Kraut, J. (1984) *J. Biol. Chem. 259*, 13027−13035.
Poulos, T. L., Edwards, S. L., Wariishi, H., & Gold, M. H. (1993) *J. Biol. Chem. 268*, 4429−4440.
Sandstrom, J. (1982) *Dynamic NMR Spectroscopy*, Academic Press, London.
Satterlee, J. D. (1986) in *Annual Report on NMR Spectroscopy* (Webb, G. A., Ed.) Vol. 17, pp 79−178, Academic Press, London.
Satterlee, J. D., & Erman, J. E. (1981) *J. Biol. Chem. 256*, 41091−1093.
Satterlee, J. D., & Erman, J. E. (1991) *Biochemistry 30*, 4398−4405.
Satterlee, J. D., Alam, S. L., Mauro, J. M., Erman, J. E., & Poulos, T. L. (1994) *Eur. J. Biochem. 224*, 81−87.
States, D. J., Haberkorn, R. A., & Reuben, D. J. (1982) *J. Magn. Reson, 48*, 286−292.
Spencer, R. G. S., Horska, A., Ferretti, J. A., & Weiss, G. H. (1993) *J. Magn. Reson. Ser B 101*, 294−296.
Summers, F. E., & Erman, J. E. (1988) *J. Biol. Chem. 263*, 14267−14275.
Sundaramoorthy, M., Kishi, K., Gold, M. H., & Poulos, T. L. (1994) *J. Biol. Chem.* 32759−32767.
Yi, Q., Alam, S. L., Satterlee, J. D., & Erman, J. E. (1993) in *Techniques in Protein Chemistry IV* (Angeletti-Hogue, R., Ed.) pp 605−613, Academic Press, New York.
Yi, Q., Erman, J. E., & Satterlee, J. D. (1994) *J. Am. Chem. Soc. 116*, 1981−1987.

BI951218E